

SOME REGULARITIES OF THE TURBULENT PRESSURE
FIELD IN THE BOUNDARY LAYER ON A FLAT PLATE

A. V. Smol'yakov

In this paper we present the results of calculations of the space correlations of the random pressure field which acts on the surface of a flat plate out of a fully developed turbulent boundary layer. Calculations are performed on the basis of available experimental data on the cross-spectral density of the turbulent pressure fluctuations. It is found that the space-time correlations have an explicitly expressed form similarity. This is used as a basis for deriving a simple approximate relation between the modulus of the normalized cross-spectral density, the energy spectrum, and the maxima of the space-time correlation coefficient. The results of elementary calculations performed on the basis of the obtained relation are shown to be almost identical with those obtained on a digital computer from exact formulas.

1. The solution of numerous problems requires information on various statistical characteristics of the turbulent boundary layer, which include the characteristics of the turbulent pressure field. Among such problems are the aerodynamic noise generated by the boundary layer during the motion of flight vehicles [1, 2], the buildup of vibrations in elastic structures situated in a flow [3, 4], the generation of wind-waves at the free surface of a fluid [5], and many others. Furthermore, knowledge of the statistical characteristics of the pressure field is required for better understanding of the structure of the turbulent boundary layer. The subject of theoretical and experimental investigations in incompressible fluid boundary layers is frequently a complex function, namely the cross-spectral density of pressure fluctuations at the plate surface:

$$P(\xi, \omega) = \frac{1}{2\pi} \int_{-\infty}^{\infty} R(\xi, \tau) \exp(-i\omega\tau) d\tau \quad (1.1)$$

where $R(\xi, \tau) = \langle p(\mathbf{x}, t) p(\mathbf{x} + \xi, t + \tau) \rangle$ is the space-time correlation of fluctuations of pressure p in a field stationary with respect to time t and uniform with respect to space \mathbf{x} ; ξ and τ are the spatial (in the plane of the plate) and the time interval between the observation points, respectively; and ω is the angular frequency of the pulsations. The fact that among all the statistical characteristics the cross-spectral density is particularly appealing to investigators may be attributed to the possibility of it being measured with minimum distortion [6].

However, in the solution of actual problems associated with turbulent pressures, it is frequently more convenient to possess information on the correlations $R(\xi, \tau)$ rather than on the cross-spectral density. In principle, it is always possible to calculate $R(\xi, \tau)$ from the known function $P(\xi, \omega)$ with the aid of Fourier transforms inverse to (1.1),

$$R(\xi, \tau) = \int_{-\infty}^{\infty} P(\xi, \omega) \exp(i\omega\tau) d\omega \quad (1.2)$$

Such calculations, however, are extremely cumbersome, and the use of a computer is unavoidable whenever $R(\xi, \tau)$ has to be determined for a wide range of ξ and τ .

Leningrad. Translated from *Zhurnal Prikladnoi Mekhaniki i Tekhnicheskoi Fiziki*, Vol. 10, No. 3, pp. 116-120, May-June, 1969. Original article submitted October 21, 1968.

© 1972 Consultants Bureau, a division of Plenum Publishing Corporation, 227 West 17th Street, New York, N. Y. 10011. All rights reserved. This article cannot be reproduced for any purpose whatsoever without permission of the publisher. A copy of this article is available from the publisher for \$15.00.

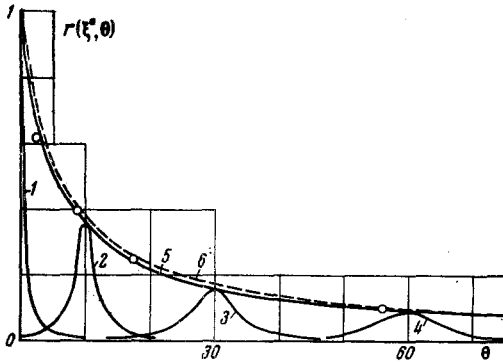


Fig. 1. Coefficient of longitudinal spatial correlations; curves 1, 2, 3, 4, and 5, correspond to exact computer calculations from formula (1.2) for $\xi^\circ = 0.10, 30, 60,$ and $\xi^\circ = \theta$, respectively; the open circles correspond to approximate calculations from formula (3.4) and spectrum (2.3); curve 6 corresponds to approximate calculations from formula (4.2) and spectrum (4.1).

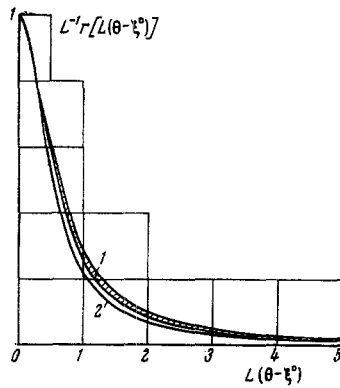


Fig. 2. Similarity of the space-time correlations; curve 1 corresponds to exact computer calculations for the range $\xi^\circ = 0-120$; curve 2 corresponds to approximate calculations from formula (4.3).

Here δ^* is the boundary layer displacement thickness, and $\langle p^2 \rangle$ is the dispersion of turbulent pressure pulsations at the plate surface.

The energy spectrum (2.3) and the cross-spectral density (2.1) for $\alpha = 0.088$ were used to calculate the longitudinal ($\eta = 0$) space-time correlations from formula (1.2) with the aid of a "Promin" digital computer. Automatic sampling (for each value of ξ and τ) was programmed for an integration step for which the error of the trapezoidal rule did not exceed 0.5%. The upper and lower bounds of integration were selected from the condition of achieving machine zero for the cross-spectral density. Some of the computed results are shown in Fig. 1. It may be seen from the curves that the peak values of the correlation coefficients

But there exists another approach, by means of which fairly simple approximate expressions can be obtained, whose accuracy is nevertheless quite satisfactory. In the following, it will be shown that this is possible due to the existence of a specific relationship between the energy spectrum and the modulus of the cross-spectral density of turbulent pressures.

2. In the following we use an expression for the cross-spectral density in a form proposed by Corcos [7]:

$$\frac{P(\xi, \omega)}{P(0, \omega)} = A \left(\frac{\xi \omega}{U_0} \right) B \left(\frac{\eta \omega}{U_0} \right) \exp \left(-i \frac{\varepsilon \omega}{U_0} \right) \quad (2.1)$$

where $P(0, \omega)$ is the spectral energy density of the turbulent pressure pulsations (or the cross-spectral density for a zero spatial interval); ξ and η are the components of vector ξ that are parallel and perpendicular to the direction of the averaged flow velocity in the boundary layer, respectively; A and B are the moduli of the normalized longitudinal and transverse cross-spectral densities, respectively; and U_0 is the phase velocity of the corresponding frequency component of the pressure field.

Numerous measurements performed by various investigators [8-10] justify the use of representation (2.1), at least for a wide range of ξ and ω . The moduli A and B measured are satisfactorily approximated by the exponential functions

$$A = \exp \left(-\alpha \frac{|\xi| \omega}{U_0} \right), \quad B = \exp \left(-\beta \frac{|\eta| \omega}{U_0} \right) \quad (2.2)$$

and although the values of α , β , and U_0 differ somewhat in the various tests, the data spread is moderate and the data may be assumed to concentrate in the intervals $\alpha = 0.08$ to 0.10 , $\beta = 0.55$ to 0.60 , and $U_0 = (0.7-0.8) U_1$, where U_1 is the averaged flow velocity at the outer edge of the boundary layer.

Extremely thorough measurements of the energy spectrum $P(0, \omega)$ of the pressure pulsations on a flat plate have been performed, in particular, by Willmarth and Wooldridge [11] and by Willmarth and Roos [8]. The data on the energy spectrum obtained in [8] are generally considered to be highly reliable. The analytical expression

$$\Pi(\Omega) = \frac{P(0, \Omega) U_1}{\langle p^2 \rangle \delta^*} = \frac{1.27}{1 + \exp(1.237 \Omega^{0.625})} \Omega = \frac{\omega \delta^*}{U_1} \quad (2.3)$$

provides a good approximation to the data [8].

$$L(\xi^{\circ}) = \frac{1}{\langle p^2 \rangle} R\left(\xi, \tau = \frac{\xi}{U_0}\right), \quad \xi^{\circ} = \frac{\xi U_1}{\delta^* U_0} \quad (2.4)$$

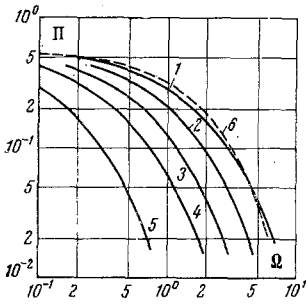


Fig. 3. Curves 1, 2, 3, 4, and 5 correspond to $L = 1.0, 0.63, 0.40, 0.25, 0.10$; curve 6 corresponds to the exponential spectrum (4.1).

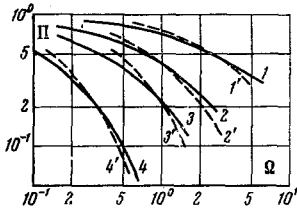


Fig. 4. Curves 1, 2, 3, and 4 correspond to the left-hand side of (3.4) for $L = 0.63, 0.40, 0.25, 0.10$; curves 1', 2', 3', and 4' correspond to $\exp(-0.088 \Omega |\xi^{\circ}|)$ for $\xi^{\circ} = 2.5, 9.0, 17.5, 56.0$.

first increase rapidly and then diminish slowly with increasing distance ξ° between the observation points, the correlation functions growing more and more shallow. All this is in good agreement with direct correlation measurements [11]. The fact that the areas below the curves $r(\xi, \tau) = \langle p^2 \rangle^{-1} R(\xi, \tau)$ are not alike is not surprising, since it is a direct consequence of the representation of the cross-spectral density in the form of (2.1) [7]. Much more unexpected is the similarity of the shape of the space-time correlations for arbitrary values of ξ° and $\theta = \tau U_1 / \delta^*$. In spite of it being clearly seen in Fig. 2, this fact could not be predicted a priori. The reason for this surprising result will be explained below, but its exceptional usefulness should be noted at this point. It consists in the fact that in order to plot the entire family of $R(\xi, \tau)$ curves, there is apparently no need to introduce Fourier transforms (1.2) for all the possible combinations of ξ and τ . It is sufficient to set $\tau = \xi / U_0$, thereby defining the shape of the curve $L(\xi^{\circ})$ for the peaks of the family $\langle p^2 \rangle^{-1} R(\xi, \tau)$; on the other hand, any of the curves of this family can be readily obtained from the autocorrelation*

$$R(0, \tau) = \int_0^{\infty} P(0, \omega) \exp(i\omega\tau) d\omega \quad (2.5)$$

by affine transformation of the coordinates with the aid of the scale $L(\bar{\xi})$

$$R(\bar{\xi}, \tau) = LR[0, L(\tau - \bar{\xi} / U_0)] \quad (2.6)$$

3. Formula of the Spectral Relations Similarity (2.6) of the correlations does not derive from anywhere, and in order to understand why it is fulfilled, it is advisable to examine the inverse problem: to assume that this similarity exists and to attempt to derive from here possible consequences.

On the basis of (1.1), (2.1), and (2.6), we may write

$$\begin{aligned} P(0, \omega) A(\xi\omega / U_0) \exp(-i\omega\xi / U_0) = \\ = \frac{1}{2\pi} \int_{-\infty}^{\infty} LR[0, L(\tau - \xi / U_0)] \exp(-i\omega\tau) d\tau \end{aligned} \quad (3.1)$$

After the change of variables $\vartheta = L\tau$, $\chi = \omega / L$, the right-hand side of (3.1) takes the form

$$\frac{1}{2\pi} \int_{-\infty}^{\infty} R(0, \vartheta - L\xi / U_0) \exp(-i\chi\vartheta) d\vartheta \quad (3.2)$$

Integral (3.2) may be treated as the spectrum of a function with a time lag $\Delta\vartheta = L\xi / U_0$. As we know [12], the spectrum $P_{\Delta}(\chi)$ of the lagging function $R(\vartheta - \Delta\vartheta)$ is related to the spectrum $P(\chi)$ of function $R(\vartheta)$ by the relation

$$P_{\Delta}(\chi) = P(\chi) \exp(-i\chi\Delta\vartheta) \quad (3.3)$$

By comparing (3.1), (3.2), and (3.3), and returning to the initial variables, we arrive at the relation

$$\frac{P(0, \omega / L)}{P(0, \omega)} = A\left(\frac{\omega\xi}{U_0}\right) \quad (3.4)$$

which may be termed the formula of spectral relations. It shows that the modulus of the normalized longitudinal cross-spectral density is equal to the ratio of the energy spectrum transposed L^{-1} times in frequency with respect to the real energy spectrum.

*The value of the lower bound of the integral (2.5) takes into account that the experimentally determined spectrum $P(0, \omega)$ is "unilateral", i.e., not all the energy is assumed to be distributed solely in the region $\omega \geq 0$.

The structure of the relationship obtained, however, requires that for fixed ξ , U_0 , and L , the right- and left-hand sides of (3.4) possess the same frequency dependence. It is obvious that for arbitrary functions $P(0, \omega)$ and $A(\omega\xi/U_0)$, this requirement need not always be fulfilled. If, for example, modulus A is given in the form of the exponential curve (2.2), relation (3.4) can be rigorously satisfied only if the energy spectrum has the analytical form

$$P(0, \omega) \sim \exp(-\gamma\omega), \quad \gamma = \text{const} \quad (3.5)$$

In our case, on the basis of experimental data, we adopted relations (2.3) and (2.2), for which formula (3.4) cannot be absolutely correct. As a consequence, with respect to the data shown in Fig. 2, it may be definitely stated that in spite of the convincing matching of the curves $R(\xi, \tau)$, calculated on a computer, their similarity was not strict. Nevertheless, it is not difficult to see (Fig. 3) that spectra (2.3) and (3.5) differ only slightly. This is exactly the reason why the computed correlation functions are well described by the similarity relation (2.6). Thus, the surprising result revealed by the calculations has now found an explanation.

It may well be that the experimentally observed similarity of the functional frequency dependences of the energy spectrum and the modulus of the normalized cross-spectral density are not a mere coincidence but rather are a phenomenon caused by some intrinsic regularities of the fully developed turbulent boundary layer. It is not possible, however, to prove or refute theoretically the compulsory nature of this similarity, and for the time being it should be accepted as an experimental fact.

The significant deviation of the experimentally observed spectrum (2.3) from the exponential form (3.5) gives reason to expect that the formula of spectral relations will be satisfactorily accurate for the wall pressure field beneath the turbulent boundary layer on a flat plate. A procedure for graphically solving equation (3.4) is shown in Figs. 3 and 4 for $L = 0.63, 0.40, 0.25$, and 0.10 . It may be seen that for properly selected values of ξ° , the right- and left-hand sides of (3.4) have approximately the same frequency dependence. In Fig. 1, the values of function $L(\xi^\circ)$ determined in this way are compared with its values obtained on a computer from exact formulas. It may be seen that the accuracy of (3.4) is completely satisfactory.

4. Other Approximate Relations. If the energy spectrum is assumed to have the form (3.5), the normalization condition

$$\int_0^\infty P(0, \omega) d\omega = \langle p^2 \rangle$$

together with the requirement of the best approximation of spectrum (2.3) make it possible to determine the constants, and to write

$$\frac{P(0, \Omega) U_1}{\langle p^2 \rangle \delta^*} = 0.548 \exp(-0.548\Omega) \quad (4.1)$$

By substituting (4.1) into (3.4) for

$$A\left(\frac{\omega\xi}{U_0}\right) = \exp\left(-\alpha \frac{|\xi| \omega}{U_0}\right) = \exp(-\alpha\Omega |\xi^\circ|)$$

we obtain a simple analytical expression for the peak values of the coefficient of the longitudinal space-time correlation

$$L(\xi^\circ) = \left(1 + \frac{\alpha |\xi^\circ|}{0.548}\right)^{-1} \quad (4.2)$$

In Fig. 1, it is shown that relation (4.2) is very close to the exact relation, if, as before, $\alpha = 0.088$.

It is not difficult to obtain an expression for the longitudinal space-time correlations

$$\begin{aligned} \frac{1}{\langle p^2 \rangle} R(\xi, \tau) &= \frac{0.548\delta^*}{U_1} \int_{-\infty}^{\infty} \exp\left[-\Omega(0.548 + \alpha |\xi^\circ|) - i\omega\left(\frac{\xi}{U_0} - \tau\right)\right] d\omega \\ &= \frac{0.548(0.548 + \alpha |\xi^\circ|)}{(0.548 + \alpha |\xi^\circ|)^2 + (0 - |\xi^\circ|)^2} \end{aligned} \quad (4.3)$$

whence the autocorrelation coefficient is

$$\frac{1}{\langle p^2 \rangle} R(0, \tau) = \left[1 + \left(\frac{\theta}{0.548} \right)^2 \right]^{-1} \quad (4.4)$$

It can be readily seen that (4.3) can be obtained from (4.4) by affine transformation of (2.6) with the aid scale (4.2). In Fig. 2, the exact values of the space-time correlations are compared with the approximate values from (4.3). The comparison reveals a small difference between the exact and approximate results.

The functions $R(\xi, \tau)$ were calculated on a digital computer for the vector intervals $\xi(\xi, \eta)$ at $\eta = 0$. However, by satisfying the accuracy of the analytical relations based on the use of the energy spectrum (4.1), cumbersome computations can be avoided. On the basis of (2.1) and (2.2), relation (4.3) can be readily generalized to the form

$$\frac{1}{\langle p^2 \rangle} R(\xi, \eta, \tau) = \frac{0.548 (0.548 + \alpha |\xi^\circ| + \beta |\eta^\circ|)}{(0.548 + \alpha |\xi^\circ| + \beta |\eta^\circ|)^2 + (\theta - |\xi^\circ|)^2} \quad (4.5)$$

$(\bar{\eta}^\circ = \eta U_1 / \delta^* U_0)$

This makes it possible to characterize in correlative terms the statistical properties of the random turbulent pressure field on a flat plate. The accuracy of (4.5) and (4.3) is alike, since both are derived under the same assumptions.

The author is indebted to Yu. G. Blyudze for useful discussions of the results of this paper.

LITERATURE CITED

1. M. J. Lighthill, "On sound generated aerodynamically, pt. 11: Turbulence as a source of sound," Proc. Roy. Soc. Lond., ser. A, vol. 222, no. 1148, 1954.
2. Random Vibration, Vol. 2, Massachusetts, 1963.
3. J. Dyer, "Response of plates to a decaying and convecting random pressure field," J. Acoust. Soc. America, vol. 31, no. 7, 1959.
4. L. Maestrello, "Use of turbulent model to calculate the vibration and radiation responses of a panel, with practical suggestions for reducing sound level," J. Sound and Vibrat., vol. 5, no. 3, 1967.
5. O. M. Phillips, "On the generation of waves by turbulent wind," J. Fluid Mech., vol. 2, no. 5, 1957.
6. G. M. Corcos, "The structure of the turbulent pressure field in boundary layer," J. Fluid Mech., vol. 18, no. 3, 1964.
7. G. M. Corcos, "Resolution of pressure in turbulence," J. Acoust. Soc. Amer., vol. 35, no. 2, 1963.
8. W. W. Willmarth and F. W. Roos, "Resolution and structure of the wall pressure field beneath a turbulent boundary layer," J. Fluid Mech., vol. 22, no. 1, 1965.
9. M. K. Bull, "Wall - pressure fluctuations associated with subsonic turbulent boundary layer flow," J. Fluid Mech., vol. 28, no. 4, 1967.
10. G. F. Carey, J. E. Chlupsa, and H. Schloemer, "Acoustic turbulent water - flow tunnel," J. Acoust. Soc. America, vol. 41, no. 2, 1967.
11. W. W. Willmarth and C. E. Wooldridge, "Measurements of the fluctuating pressure at the wall beneath a thick turbulent boundary layer," Fluid Mech., vol. 14, no. 1, 1962.
12. A. A. Kharkevich, Spectra and Analysis [in Russian], Fizmatgiz, Moscow, 1962.